Ultrafast Evolution of the Excited-State Potential Energy Surface of TiO_2 Single Crystals Induced by Carrier Cooling

Elisabeth M. Bothschafter,[1,2,*] Alexander Paarmann,[3] Eeuwe S. Zijlstra,[4] Nicholas Karpowicz,[2] Martin E. Garcia,[4] Reinhard Kienberger,[1,2] and Ralph Ernstorfer[3,†]

[1]*Technische Universität München, Physik-Department, James-Franck-Straße, 85748 Garching, Germany*
[2]*Max-Planck-Institut für Quantenoptik, Hans-Kopfermann-Straße 1, 85748 Garching, Germany*
[3]*Fritz-Haber-Institut der Max-Planck-Gesellschaft, Faradayweg 4-6, 14195 Berlin, Germany*
[4]*Universität Kassel, Theoretische Physik, Heinrich-Plett-Strasse 40, 34132 Kassel, Germany*

(Received 15 August 2012; published 7 February 2013)

We investigate the influence of carrier cooling dynamics in TiO_2 on the excited-state potential energy surface along the A_{1g} optical phonon coordinate after above band-gap excitation using ultrashort ultraviolet pulses. The large amplitude coherent oscillation observed in a pump-probe transient reflectivity measurement shows a phase shift of -0.2π with respect to a purely instantaneous displacive excitation. The dynamic evolution of the potential energy surface minimum of the coherent phonon coordinate is explored using accurate density functional theory calculations, which confirm a shift of the potential energy surface minimum upon resonant laser excitation and reveal a significant positive contribution to the displacive force due to the cooling of the excited hot electron-hole plasma. We show that this noninstantaneous effect can quantitatively explain the experimentally observed phase using reasonable assumptions for the parameters characterizing the excited carriers. Our work demonstrates that the fast equilibration dynamics of laser-excited nonequilibrium carrier populations can have a pronounced effect on the initial structural response of crystalline solids.

DOI: 10.1103/PhysRevLett.110.067402 PACS numbers: 78.47.jg, 63.20.kd, 71.38.−k, 78.40.−q

The ultrafast vibrational and electronic dynamics in a solid provide valuable insight regarding the mutual dependence of atomic and electronic degrees of freedom. While time- and angle-resolved photoelectron spectroscopy [1,2] and time-resolved diffraction techniques [3–5] provide direct access to the dynamics of either electronic or atomic structures, ultrafast all-optical techniques have proven to be powerful tools for studying correlated dynamics with high time resolution. In particular, materials with strong coupling of real or virtual electronic excitation to optical phonons often exhibit a clear correlation between the atomic configuration projected on one or more phonon coordinates and the optical response [6,7]. In combination with first-principles theoretical models, the optical response of suitable systems can be well correlated with the underlying structural changes, providing a comprehensive understanding of the transient optical response [8].

The vast majority of ultrafast optical studies employ femtosecond pump pulses in the near-infrared to ultraviolet (UV) spectral range, which trigger a lattice response through real or virtual excitations. These excitations provide a time-dependent driving force $F(t)$ for one or multiple modes of the lattice, and in first approximation the phonon coordinate $Q(t)$ can be described as a driven harmonic oscillator [9,10]

$$\mu\left[\frac{\partial^2 Q(t)}{\partial t^2} + 2\beta\frac{\partial Q(t)}{\partial t} + \omega_0^2 Q(t)\right] = F(t), \qquad (1)$$

where μ is the reduced lattice mass, β describes the damping, and ω_0 is the undamped phonon frequency. The limiting case of purely real electronic excitation results in the simplest approximation in an error function-shaped $F(t)$ with its rise time and amplitude being proportional to the pump pulse duration and number of excited carriers, respectively [6]. In this case, $F(t)$ results in a shift of the minimum of the harmonic oscillator potential, which is usually referred to as displacive excitation of coherent phonons (DECP) [6]. The opposite limiting case is that of impulsively stimulated Raman scattering (ISRS) with $F(t)$ resembling the temporal profile of the pump pulse. ISRS predominates in case the optical pump pulse is nonresonant with the electronic transitions of the system. The two driving mechanisms can be distinguished through their resulting phase difference of $\pi/2$ of the coherent lattice vibrations relative to the optical excitation [9]. Both pictures have been unified by introducing a lifetime γ of the optically excited electrons with $\gamma \rightarrow \infty$ for the DECP limit and $\gamma \rightarrow 0$ for the ISRS limit [10,11], correctly describing the transient response from a macroscopic point of view.

As has been suggested before, the driving force might not only depend on the number of excited carriers but also on their temperature [6]. More generally, for a given number of excited carriers, the potential energy surface (PES) of a lattice may exhibit a profound dependence on their energetic distribution. This is of particular importance when carrier dynamics occur on time scales comparable to or shorter than the period of the generated phonon.

In such a case, $F(t)$ deviates from both limiting cases and evolves on the time scale of the phonon oscillation. Here, we provide the first experimental evidence for such a dynamic evolution of the displacive force in TiO_2 under resonant excitation. The ultrafast relaxation dynamics of carriers excited above the band-gap leads to a fast evolution of the PES minimum of the lattice, manifesting itself in an effective phase shift of the coherent phonon oscillation. Density functional theory calculations of the correlation between the excited-carrier dynamics and the lattice response reveal the role of carrier cooling and describe the underlying dynamics from a microscopic point of view.

Resonant interband excitation of electrons in TiO_2 involves a charge redistribution in real space as the valence band exhibits predominantly O $2p$ orbital character and the conduction band is of Ti $3d$ character [12]. As the PES of the lattice is a complex functional of the charge distribution, electronic excitation of TiO_2 can be expected to shift the minimum of the PES in configuration space and trigger the displacive excitation of coherent phonons. The photon energy of the UV laser pulses employed in this study significantly exceeds the band-gap of TiO_2. In combination with the extremely short pulse duration, we are able to generate highly nonequilibrium electron and hole distributions in the conduction and valence band, respectively. In a theoretical study by Zhukov and Chulkov [13], the relaxation dynamics of electrons excited well above the conduction band minimum have been studied. Except for excited states with little excess energy, relaxation times are found to be on the 10-fs time scale due to strong electron-phonon coupling [14]. Consequently, the lattice response of TiO_2 to ultrafast resonant excitation is expected to be influenced at early times by electron relaxation dynamics.

In our experiment, the transient changes in reflectivity of the rutile TiO_2 (110) surface were recorded in a one-color pump-probe scheme in parallel linear polarization along the [001] direction using the 3rd harmonic of sub-4-fs, 400 μJ near-infrared pulses, generated in neon. The UV pulses are centered at 245 nm with a spectral width (full width at half-maximum) of 40 nm, corresponding to a Fourier limit below 3 fs [15]. Pump fluences ranging from 0.7 to 1.3 mJ/cm^2 were employed. The best signal-to-noise ratio of the transient reflectivity signal was achieved by a delay-differential method using lock-in amplification of the delay-modulated signal [16], essentially recording the delay derivative of the reflectivity, $\delta R/\delta t$. Additionally, we also recorded the transient reflectivity $\Delta R/R_0$ directly by a rapid scanning of the delay t combined with high averaging. Upon photoexcitation, we observe a remarkable drop in reflectivity of up to 3.5%, increasing linearly with the pump fluence, and a modulation of up to 0.3% by the coherent oscillation (Fig. 1). Such a large response occurs in materials exhibiting strong charge carrier interactions and effects of a similar magnitude have been observed mainly in other transition metal oxides, e.g., in Ti_2O_3 [6] and VO_2 [17].

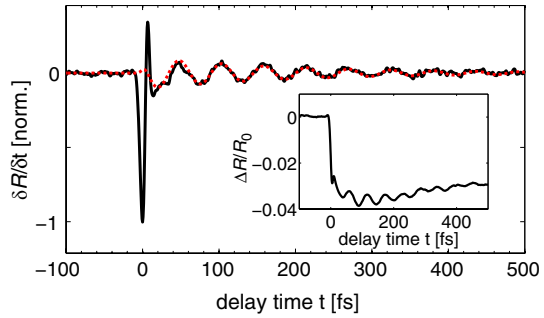

FIG. 1 (color online). Transient reflectivity of TiO_2. The delay-differential reflectivity signal $\delta R/\delta t$ is shown (black solid line), as well as the least-square fit of the coherent phonon oscillation with an exponentially decaying ($\sim$200 fs) sine function (red dotted line). The inset shows the transient reflectivity signal $\Delta R/R_0$ at 1.3 mJ/cm^2 pump fluence.

Figure 1 shows the delay-differential reflectivity signal (black solid line) and the fit to extract the phonon contribution (red dotted line). The first spike in the delay-differential signal corresponds to an initial drop in the transient reflectivity; see inset. This instantaneous drop in reflectivity is attributed to the excitation of electrons into the conduction band. The oscillation of the coherent phonon is described best by an exponentially decaying sine function $A\exp(-t/\tau)\sin(\omega t + \phi)$ in the delay-differential signal (red dotted line) with a decay time of $\tau \sim 200$ fs. The details of the data analysis are given in the Supplemental Material [18]. The results of the best fits to the data recorded with the delay-differential technique for the amplitude A, the frequency $\omega/2\pi$, and the phase ϕ of the coherent phonon contribution are shown in Fig. 2 as a function of the incident pump fluence. While the phonon amplitude increases with the pump fluence in the range of fluences applied, its frequency and phase remain unchanged. The phonon frequency of $\sim$18 THz can be assigned to the longitudinal optical phonon of rutile TiO_2 with A_{1g} symmetry [19,20].

Remarkably, the phase ϕ of the coherent phonon oscillation in the delay-differential signal is -0.2π, independent

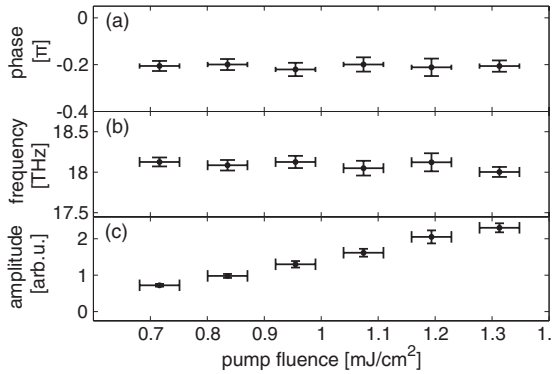

FIG. 2. Fit results of the phonons' phase (a), frequency (b), and amplitude (c) as a function of the pump fluence.

of the applied pump fluence. This corresponds to a cosine oscillation of the transient reflectivity as expected for DECP [6], however, with its maximum shifted by -0.2π. This phase shift is equivalent to a temporal delay of ~5.5 fs with respect to the time of the electronic excitation marked by the initial drop in reflectivity. While there are possible causes for observing a phase-shifted oscillation within the DECP model, e.g., phonon damping, electron-hole recombination [10], or carrier diffusion, we find that these effects are small compared to the observed phase shift; see the Supplemental Material for details [18]. We also point out that the excitation mechanism we observe under resonant excitation conditions notably differs from previous work by Nomoto *et al.* [20]. Their study found the $\chi^{(3)}$ response of the A_{1g} optical phonon to nonresonant excitation to be consistent with the ISRS generation mechanism and, consequently, a sinelike motion of the A_{1g} coherent phonon.

In order to investigate the origin of the observed phase shift and, more generally, the influence of hot carrier dynamics on the coherent phonon excitation, we conducted a microscopic modeling of TiO_2 using Wien2k [21]. Methodological details of the calculation are equivalent to Ref. [22]. To explore the structural effects arising from laser excitation, three states of the system are modeled and compared [see Fig. 3(a)]. First, we calculate the ground state of the system; the corresponding PES is shown in Fig. 3(a) as black solid line. The oxygen atom position u along the A_{1g} phonon coordinate is given in units of $\sqrt{2}a$, where $a = 4.593$ Å is the lattice parameter. The ground states' PES minimum is at $u = 0.3048$ and the curvature corresponds to an A_{1g} phonon frequency of 17.9 THz. Both results are in good agreement with experimentally determined values [19]. Since our UV photon energy of ~5.0 eV significantly exceeds the TiO_2 band-gap of ~3 eV [23], we further model two states of laser-excited TiO_2: the PES for a hot electron system with an electronic temperature of 1 eV and the PES for an electronically excited system, but thermally relaxed to room temperature; see Fig. 3(a). As the electrons and holes do not have sufficient excess energy for creating additional electron-hole pairs during scattering processes of the lowest order and as recombination occurs on a much longer time scale [13], the number of excited carriers is kept fixed at 0.1 excited electron-hole pairs per unit cell for both the hot and cold excited state. Immediately after laser excitation [vertical arrow in Fig. 3(a)], the excited electrons start to emit high-frequency phonons at a rate $>10^{14}$ s^{-1}, which results in the rapid cooling of the hot electrons in the conduction band while the number of electron-hole pairs remains unaffected [13]. Although the holes have not been treated explicitly in Ref. [13], we assumed that the holes relax at a similar rate. The theoretically determined time scale for the emission of a single phonon by an excited carrier is 2 fs [13] independent of the initial electron energy, which is in

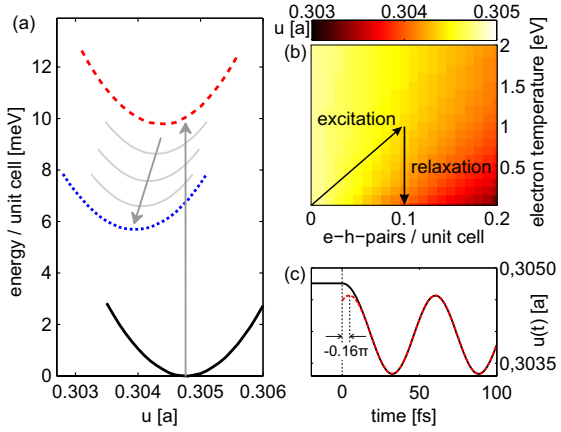

FIG. 3 (color online). (a) PES of TiO_2 along the A_{1g} phonon coordinate in the electronic ground state (black solid line), the hot laser-excited state with an electron temperature of 1 eV (red dashed line), and the cooled excited state with a temperature of 0.027 eV (blue dotted line). The excitation density of both excited states is 0.1 electron-hole pairs per unit cell, corresponding to the experimentally employed fluence regime. The PES of hot and cold excited states are offset by −414.9 and −197.3 meV, respectively, for clarity of representation. (b) Position of the PES minimum as a function of the number of excited electron-hole pairs per unit cell and the electron temperature. (c) Calculated oxygen atom trajectory (black solid line), in comparison with a cosine oscillation at 17.9 THz that perfectly describes the motion after $t = 20$ fs. This cosine oscillation exhibits a phase shift of -0.16π (red dashed line), as illustrated with the black dashed lines and black arrows, which allows us to determine the effective phase shift of the atomic motion.

agreement with time-domain THz measurements [14]. Zhukov *et al.* determined a total relaxation time of electrons with 1-eV excess energy to be ~20 fs (gray downward arrow). This leads to the cool, electronically excited state near room temperature, shown in Fig. 3(a) as a blue dotted line.

Based on the electron temperature dependence of the excited-state PES, we can establish a correlation between the experimentally accessible ultrafast phonon dynamics and the dynamical evolution of the lattice PES of TiO_2 upon photoexcitation. Before the laser excitation, the atoms are in the ground state PES minimum. Both the transition between the ground state and the hot excited state, as well as the subsequent relaxation to a cool excited state, induce a shift of the PES along the A_{1g} phonon coordinate by a similar amount in the same direction. Figure 3(b) depicts the PES minimum as a function of the electronic temperature and the number of electron-hole pairs per unit cell. As can be deduced from this 2D plot, the unidirectional shift of the PES upon excitation and subsequent relaxation is a general characteristic of TiO_2. It does not depend on the specific excitation conditions, notably the number of excited electron-hole pairs or the electron temperature, used for modeling the experiment.

The electron temperature dependence of the PES can be qualitatively understood from the spatial charge redistribution for both excited states compared to the ground state. Figure 4 shows the isosurfaces for positive (red) and negative (blue) difference in valence electron density compared to the ground state at ± 0.0005, ± 0.003, and $\pm 0.0055 e/a_0^3$ (a_0 is the Bohr radius). The charge transfer from the oxygen to the titanium atoms associated with the electronic excitation is clearly visible. Figure 4(a) reveals an increase in electron density around the titanium (green) atoms and its decrease around the oxygen atoms (yellow) for the hot excited state. This represents an effective charge transfer within the unit cell, as expected for TiO_2 upon resonant excitation [12,23]. Both the valence band as well as the conduction band have the purest O $2p$ and Ti $3d$ characters, respectively, at states near the band-gap [12,24]. Therefore, the ultrafast carrier relaxation succeeding the optical excitation further enhances the intra-unit cell charge transfer, approximately by a factor of two. This implies that the charge transfer is the driving force for the shift of the PES. We expect other transition metal complexes to exhibit similar behavior [24].

Combining the electron relaxation dynamics [13] with our PES calculations, we are able to simulate the atomic motions on the time-dependent PES. We assumed that the PES changes linearly with time between the computed limiting cases at $t = 0$ and $t = 20$ fs. After $t = 20$ fs, the estimated energy relaxation time according to Ref. [13], we assumed that the PES remains constant. The PES minimum positions for the hot and cold excited states

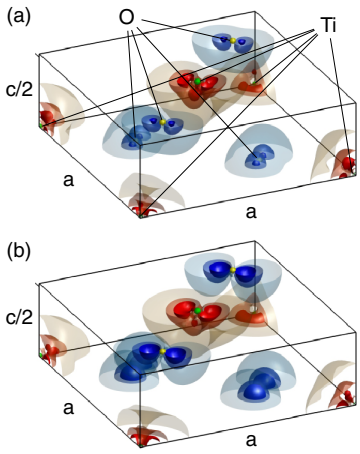

FIG. 4 (color online). Redistribution of valence electron density around oxygen (yellow) and titanium (green) atoms for hot (a) and (b) cold excited states compared to the electronic ground state, shown for one half of the unit cell. The atomic configuration is fixed at the ground state. Isosurfaces for positive (more charge, red, at Ti sites) and negative (less charge, blue, at O sites) change in charge density are shown at ± 0.0005, ± 0.003, and $\pm 0.0055 e/a_0^3$.

were taken for an electronic temperature of 1 eV and 0.1 excited electron-hole pairs; see Fig. 3(b). The motion of the oxygen atoms in the time-dependent potential was calculated by the integration of Newton's equation. While this model is rather simple, it is free of adjustable parameters. The resulting atomic motion along the A_{1g} coordinate is shown in Fig. 3(c). After $t = 20$ fs, a phase-shifted cosine oscillation with equal amplitude at 17.9 THz perfectly describes the atomic motion which allows us to determine the effective phase shift of -0.16π of the atomic motion. The agreement of this value with the experimentally observed phase shift is good evidence that the PES minimum, which determines the coherent phonon dynamics, is evolving dynamically. The magnitude of the observable phase shift of the phonon oscillation depends on two factors: (i) the amplitude ratio of the instantaneous shift of the PES minimum due to carrier excitation and the fast dynamic shift due to carrier relaxation, and (ii) the time scale of the carrier relaxation compared to the optical phonon period. In the range of excitation levels investigated experimentally, the amplitude ratio of the two contributions [see Fig. 3(b)] and the carrier relaxation time are expected to remain approximately constant. Thus, our simulation predicts the coherent oscillation to be phase-shifted by -0.16π independent of the applied fluence in good agreement with the experimental findings.

In conclusion, we have demonstrated that the rapid cooling of carriers induces an ultrafast motion of the excited-state PES in TiO_2. Resonant electronic excitation generates coherent optical phonons in TiO_2 through a displacive excitation mechanism. The phase of the coherent lattice vibration indicates a second displacive driving mechanism in addition to the prompt excitation of electron-hole pairs. Calculations of excited-state PES reveal that approximately half of the displacement originates from carrier cooling rather than excitation. While the excitation- and cooling-induced shifts of the PES in TiO_2 are unidirectional, in other materials the effect of carrier relaxation might partially compensate the excitation-induced PES shift or act on a second dimension in configuration space. Our work demonstrates that the fast equilibration dynamics of laser-excited nonequilibrium carrier populations alone can induce a significant structural response of crystalline solids. While the magnitude and dynamics of this effect will depend on the specifics of the electronic structure and electron-lattice interactions of a given material, we expect it to be general, for instance, for a range of transition metal oxides. We suggest the structural effect of carrier redistribution dynamics to be considered for resonant photo-induced processes, in particular for laser-induced ultrafast phase transitions.

N. K. gratefully acknowledges support from the Alexander von Humboldt Foundation. R. K. gratefully acknowledges an ERC starting grant.

*elisabeth.bothschafter@tum.de
†ernstorfer@fhi-berlin.mpg.de

[1] T. Hertel, E. Knoesel, M. Wolf, and G. Ertl, Phys. Rev. Lett. **76**, 535 (1996).
[2] F. Schmitt, P. S. Kirchmann, U. Bovensiepen, R. G. Moore, L. Rettig, M. Krenz, J.-H. Chu, N. Ru, L. Perfetti, D. H. Lu *et al.*, Science **321**, 1649 (2008).
[3] R. J. D. Miller, R. Ernstorfer, M. Harb, M. Gao, C. T. Hebeisen, H. Jean-Ruel, C. Lu, G. Moriena, and G. Sciaini, Acta Crystallogr. Sect. A **66**, 137 (2010).
[4] T. Elsaesser and M. Woerner, Acta Crystallogr. Sect. A **66**, 168 (2010).
[5] D. M. Fritz, D. A. Reis, B. Adams, R. A. Akre, J. Arthur, C. Blome, P. H. Bucksbaum, A. L. Cavalieri, S. Engemann, S. Fahy *et al.*, Science **315**, 633 (2007).
[6] H. J. Zeiger, J. Vidal, T. K. Cheng, E. P. Ippen, G. Dresselhaus, and M. S. Dresselhaus, Phys. Rev. B **45**, 768 (1992).
[7] M. Hase, M. Kitajima, A. Constantinescu, and H. Petek, Nature (London) **426**, 51 (2003).
[8] E. S. Zijlstra, L. L. Tatarinova, and M. E. Garcia, Phys. Rev. B **74**, 220301(R) (2006).
[9] T. Dekorsy, G. Cho, and H. Kurz, *Light Scattering in Solids VIII*, Topics in Applied Physics Vol. 76 (Springer, Berlin, 2000), pp. 169–209.
[10] D. M. Riffe and A. J. Sabbah, Phys. Rev. B **76**, 085207 (2007).
[11] T. E. Stevens, J. Kuhl, and R. Merlin, Phys. Rev. B **65**, 144304 (2002).
[12] M. Landmann, E. Rauls, and W. G. Schmidt, J. Phys. Condens. Matter **24**, 195503 (2012).
[13] V. P. Zhukov and E. V. Chulkov, J. Phys. Condens. Matter **22**, 435802 (2010).
[14] E. Hendry, F. Wang, J. Shan, T. Heinz, and M. Bonn, Phys. Rev. B **69**, 081101(R) (2004).
[15] E. M. Bothschafter, A. Schiffrin, V. S. Yakovlev, A. M. Azzeer, F. Krausz, R. Ernstorfer, and R. Kienberger, Opt. Express **18**, 9173 (2010).
[16] A. Taylor, D. Erskine, and C. Tang, Chem. Phys. Lett. **103**, 430 (1984).
[17] S. Wall, D. Wegkamp, L. Foglia, K. Appavoo, J. Nag, R. F. Haglund, J. Stähler, and M. Wolf, Nat. Commun. **3**, 721 (2012).
[18] See Supplemental Material at http://link.aps.org/supplemental/10.1103/PhysRevLett.110.067402 for details of the experiment, the data analysis, and the calculations, as well as a discussion of possible phonon phase shift contributions.
[19] C. Lee, P. Ghosez, and X. Gonze, Phys. Rev. B **50**, 13379 (1994).
[20] T. Nomoto, A. Sasahara, and H. Onishi, J. Chem. Phys. **131**, 084703 (2009).
[21] P. Blaha, K. Schwarz, G. Madsen, D. Kvasnicka, and J. Luitz, *WIEN2k, an Augmented Plane Wave + Local Orbitals Program for Calculating Crystal Properties* (Technische Universitaet Wien, Austria, 2001).
[22] M. S. Diakhate, E. S. Zijlstra, and M. E. Garcia, Appl. Phys. A **96**, 5 (2009).
[23] L. Chiodo, J. M. García-Lastra, A. Iacomino, S. Ossicini, J. Zhao, H. Petek, and A. Rubio, Phys. Rev. B **82**, 045207 (2010).
[24] P. I. Sorantin and K. Schwarz, Inorg. Chem. **31**, 567 (1992).